Chapter 1
Historical Background and Introduction

Jean-Claude Vial

Protubérances: "Ces amas de matière lumineuse ayant une grande vivacité et possédant une activité photogénique très remarquable" (A. Secchi "Le Soleil", 1877, I. 385)
Prominences: "These masses of luminous matter with a high brilliance and with a very remarkable photogenic activity"

Abstract Forty and twenty years after the two books published by Einar Tandberg-Hanssen (Solar prominences (Geophysics and astrophysics monographs), Vol. 12. Dordrecht: D. Reidel Publishing Co., 1974; The nature of solar prominences, astrophysics and space science library, Vol. 199. Dordrecht: Kluwer Academic Publishers, 1995) on solar prominences, it is time to update our knowledge and understanding of these fascinating solar structures. After a brief history which overviews first eclipse observations (drawings and then photography), spectrographic, coronagraphic and later on polarimetric measurements, the chapter presents samples of the most spectacular results of the last two decades, obtained whether from space or on the ground. It discusses the contents of the book in order to encourage the reader to dip into the following 17 chapters which provide comprehensive and detailed observations, information about the methods used, and interpretation of the results on the basis of the latest theoretical and modelling works.

1.1 A Brief History

1.1.1 The Era of Eclipses

In his book (Solar Prominences 1974), Tandberg-Hanssen (1974) traced back the first observations of prominences to the eclipse of 1239 when an observer, Muratori, reported a "burning hole" in the corona. Since then, strange structures were seen

J.-C. Vial (✉)
Université Paris-Sud & CNRS, Institut d'Astrophysique Spatiale, Orsay, France
e-mail: jean-claude.vial@ias.u-psud.fr

J.-C. Vial, O. Engvold (eds.), *Solar Prominences*, Astrophysics and Space Science Library 415, DOI 10.1007/978-3-319-10416-4_1

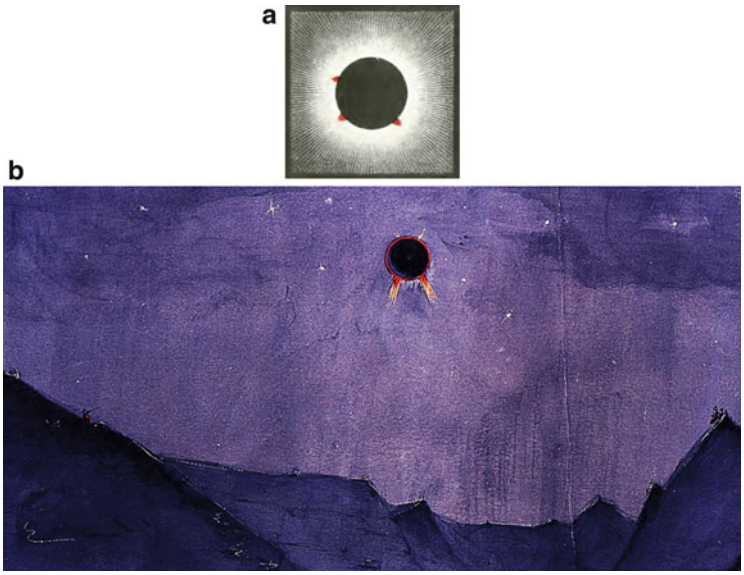

Fig. 1.1 (**a**) Drawing by the English astronomer Baily during the solar eclipse of 1842 (reproduced by A. Secchi, Le Soleil, I, p. 310). (**b**) Engraving made by Eugene Bouvard during the 1842 eclipse at Digne (France) (courtesy S. Koutchmy)

during total solar eclipses, labelled "burning holes", "red flames", ... sometimes thought to be clouds or mountains on the Moon (Vassenius 1733).

Clever observers had time to make drawings which are valuable records of the state of the solar corona at the time of the eclipse (see Fig. 1.1a where prominences are the red off-the-limb structures). But during the eclipse of July 8, 1842, as mentioned by A. Secchi, observers were so surprised by these pink colored structures that some confusion followed, where observers, such as Airy, Arago or Baily saw different structures at different locations! (see Fig. 1.1b). Some observers even considered them to be the result of optical illusions! After the 1851 eclipse in Sweden, it was admitted that these bright pieces were clouds (i.e. gases), but clouds truly belonging to the Sun ... or to the Moon? However, most observers (A. Secchi being at the forefront) noticed the change of altitude of the structures during the motion of the Moon, which they interpreted as proof that they were not attached to the Moon.

Moreover, we have evidence that when the 1851 eclipse passed over southern Scandinavia on July 28, the observers working for Airy in Oslo, Norway and in Gothenburg, Sweden, actually discovered the eruption of a prominence (Fig. 1.2, top). Compare this one and a half centuries-old observation with a modern observation showing in great details the coronal environment of prominences (Fig. 1.2, bottom).

A major step forward occurred in 1860 with the use of photography, which allowed for a permanent and "objective" record of these structures. Photography

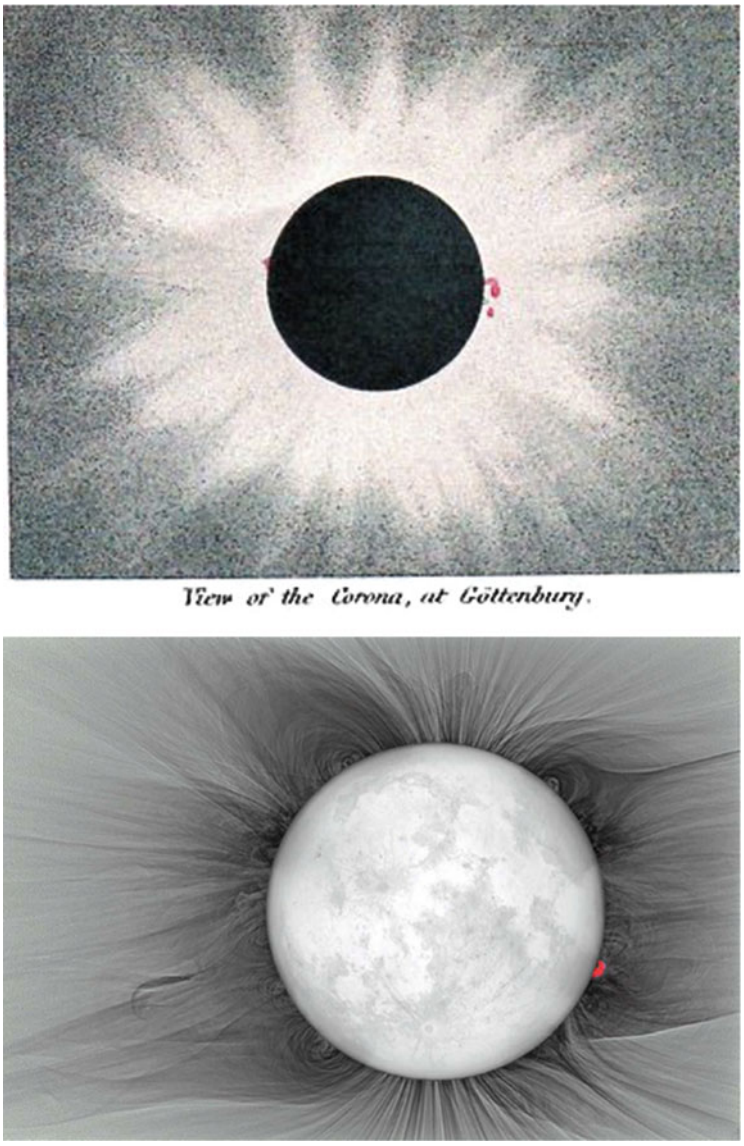

Fig. 1.2 *Top*: view of the corona and a prominence whose shape is known to be typical for erupting during the July 28, 1851 eclipse at Gothenburg, Sweden. The observer was working for Airy (courtesy O. Engvold). *Bottom*: Image taken during the total solar eclipse of 11 July 2010. The dark hook-shaped feature on the east limb is part of an erupting prominence. One prominence at the west limb is shown in *red*. Note the helmet coronal structuring above prominences. Eclipse image, courtesy of Prof. M. Druckmüller and S. Habbal

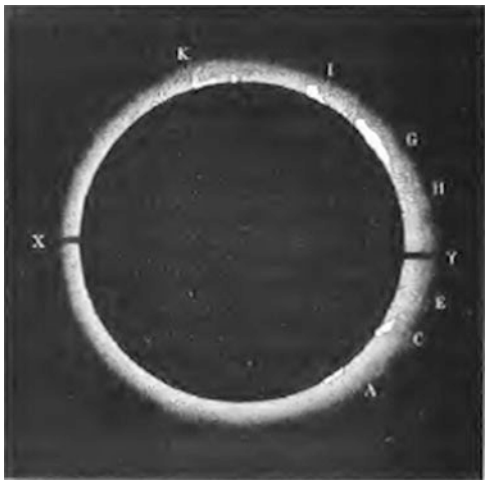

Fig. 1.3 Photograph of the eclipse of 1860 at the Desertios de las Palmas by A. Secchi (Le Soleil, I, p. 378). At least seven structures were detected

even allowed observations of prominences that were invisible to the naked eye (Fig. 1.3). The observers derived important parameters such as the shape, altitude, emissivity and also noticed that these structures were mostly connected to an underlying layer (to be identified later as the chromosphere).

At that time, photography did not provide colours, so it was important to visually observe prominences. Their commonly adopted colour was red with some mixture of violet that A. Secchi compared to the colour of the peach tree flower. Some yellow colour was occasionally noticed at the prominence tops.

1.1.2 The Use of the Spectroscope

Another important advance was achieved with spectral analysis (the foundations had been built by Bunsen and Kirchhoff) of the emitting gases.

Spectroscopes were used during the 1868 eclipse, with their slits being placed on the observed prominences, and the presence of emission lines (a hydrogen line in particular) confirmed the gaseous nature of prominences (Fig. 1.4).

But, since the observers had no wavelength scale, there still were some uncertainties concerning the identification of these lines. Should the observers wait for the next eclipse? No, the day after, J. Janssen carefully positioned the slit of his spectroscope on an off-limb suspected structure and confirmed the presence of the two lines of hydrogen (C and F) and later the D lines (two from Sodium and a mysterious third one corresponding to an unknown element). This element corresponding to the third D3 line observed for the first time in prominences was coined Helium (Helios is the Sun God in Greek) because of its solar origin. It was detected in the Earth's atmosphere 27 years later. It was identified as atomic number 2, the most abundant element in the Universe after Hydrogen.

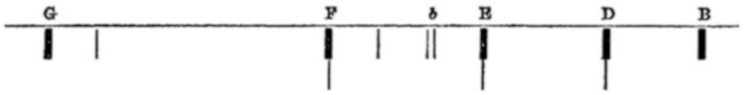

Fig. 1.4 Prominence spectrum obtained by G. Rayet (the Astronomer well-known for the Wolf-Rayet stars) during the eclipse of 1868 in Malaisia (Rayet 1869). The spectrum is marked by emission lines. The letters correspond to the Fraunhofer classification where the F line is the Hβ line of hydrogen

In "Le Soleil" (1877, II.1), Secchi wrote: "L'éclipse de 1868 sera une date mémorable dans l'histoire de l'Astronomie car c'est alors que M. Janssen apprit aux savants à étudier en tous temps les protubérances" or "The 1868 eclipse will remain a never-to-be-forgotten date in the history of Astronomy for this is when M. Janssen taught scientists how to study prominences for all times". Since then the spectroscope was used daily for the study of prominences in two different modes: a narrow slit allowing for spectroscopy and a wide slit allowing for monochromatic imaging. This means that actually the issue of spectro-imaging was already discussed and solved by observers of that time!

Moreover, the observations being more systematic over a longer period of time, it was noticed that the number and the position of prominences varied with solar activity. Classifications appeared (see Engvold 2014), mostly based upon their shapes and the proximity of active regions.

In spite of the progress brought by photography and spectrography, some observers continued visual observations. One of them, Prof. C. Fearnley in Oslo, recorded the images on black paper (Fig. 1.5). Note the delicate thread structuring, today called "fine structure".

Early observers (e.g. Vassenius 1733) had not only noted the (red) emission but also its temporal variation in prominence, which explains the use of terms such as "red flames" to characterize them. A. Secchi (Le Soleil, II. p. 42) mentions "the velocity of their motions when they are submitted to an eruptive force which launches them from the interior above the surface of the Sun". Observers were amazed by the altitude that these structures could reach (up to 250 arcsec above the limb) and already wondered about the nature of the force driving the material. Actually, what they were observing was the eruption of prominences, often above active regions, for which velocities of 100 km/s (or more) were measured with the use of a chronometer. The magnitude of the velocities even led A. Secchi (Le Soleil, II, p. 108) to raise questions that we think to be still valid today: "The nebulous masses are so quickly illuminated and they disappear within such a short time that one wonders whether it is a temporary transformation instead of an actual transport of mass".

The observers also measured the width of the line profiles from which they coarsely derived some temperatures.

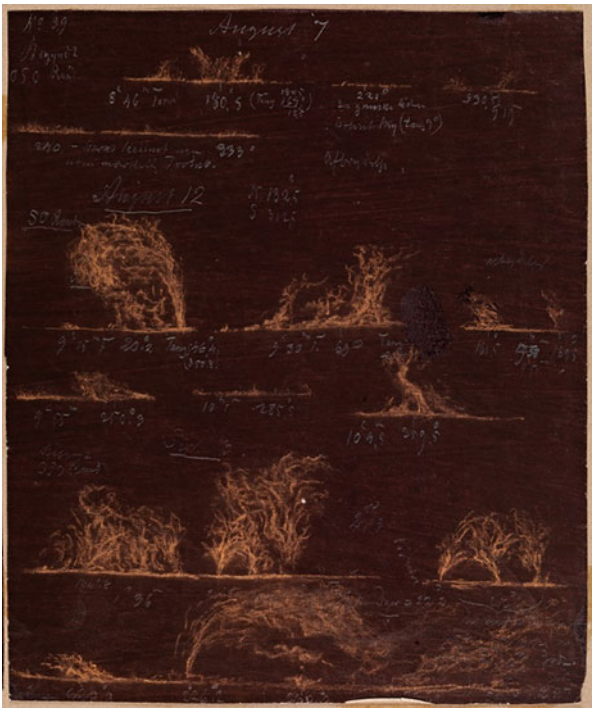

Fig. 1.5 An example of the chalk drawings made by Prof. C. Fearnley between 1871 and 1873 in Oslo, with a wide slit spectrohelioscope. Note the large variety of morphological structures (Courtesy O. Engvold)

1.1.3 Identification of Prominences Observed at the Limb with Structures Observed on the Disk

The observers moved the (wide) slit of the spectroscope around the limb which allowed them to build an image within an hour (Fig. 1.6). Systematic observations between 1871 and 1876 allowed the detection of a correlation between some prominences and the proximity of sunspots on one hand, and the declining number of prominences when the minimum of solar activity was reached (in 1875) on the other hand. Moreover, observers such as A. Secchi already classified prominences as steady (to be named "quiescent", later on) and active (to be named "active region prominences" later) (see Engvold 2014).

However, a precise identification of off-limb prominences with on-disk structures was not possible until the use of spectroheliographs allowing the isolation of (cool) chromospheric lines, called "black lines", such as the Hβ of hydrogen and the UV H and K lines of ionized calcium (Hale and Ellerman 1903 at Yerkes Observatory with a 1.05 m refractor, and Deslandres 1910 at Meudon Observatory initially with a 0.3 m mirror). It was then realized that the dark elongated features (called "elongated dark flocculi") were the very same ones than the off-limb prominences seen bright on the dark sky background. They were called *filaments* (Fig. 1.7). With the simple use of the third law of Kirchhoff, one could already derive that the temperature of

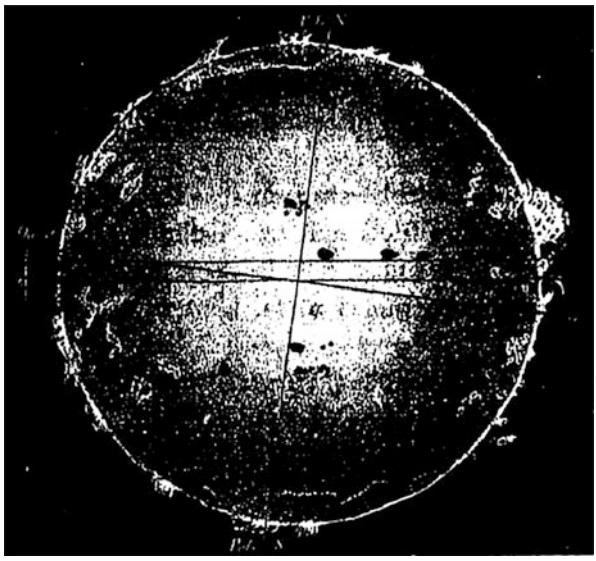

Fig. 1.6 The composite of limb drawings obtained with the wide slit spectroscope combined with disk drawings depicting sunpots and faculae (Secchi, Le Soleil, II, p. 164)

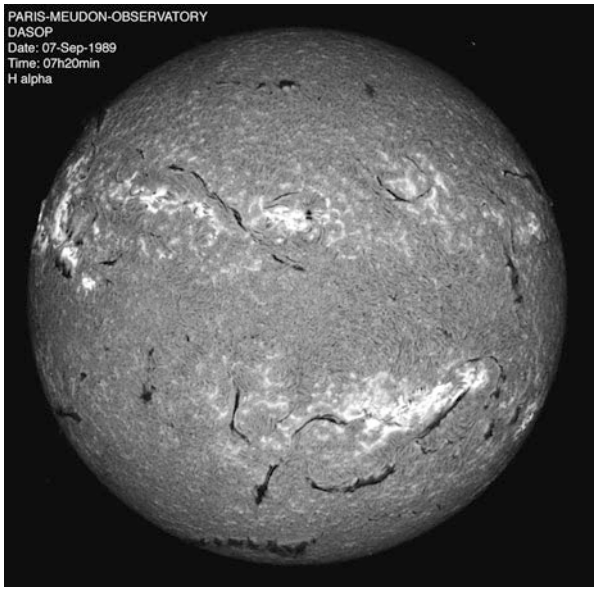

Fig. 1.7 Spectroheliogram in the Hα line obtained at Paris-Meudon Observatory. The dark elongated structures seen on the disk, called filaments, will appear as prominences when, rotating with the sun, they reach the limb (courtesy LESIA/Observatoire de Paris/CNRS/UPMC/Univ. Paris Diderot/)

the filament which acts as a screen between the chromosphere and the observer is lower than the temperature of the emitting chromosphere (10^4 K).

The systematic recording of K3 and Hα spectroheliograms at Meudon Observatory from 1919 to 1930–1937 has led to an impressive body of synoptic data from which many spatial and statistical characteristics have been derived (D'Azambuja and D'Azambuja 1948). An excellent example is provided by the study of the

law of rotation of filaments as a function of latitude (Fig. 25 of D'Azambuja and D'Azambuja 1948) which is an accurate proof of the solar differential rotation. Similar observations and identifications were made in the mm radio domain by Khangil'din (1964) who stated that "the presence of local regions of reduced radio brightness above dark filaments is established". According to Schmahl et al. (1981) two-thirds of the radio depressions are associated with Hα filaments.

1.1.4 A Major Instrumental Progress for Continuously Observing Prominences: The Coronagraph

The slit of the spectroscope allowed the observer to "ignore" the considerably stronger emission from the solar disk. But if one wanted to have an instantaneous picture of the whole corona (including prominences), as is possible during eclipses, it was necessary to block the light from the disk. This was the idea of Bernard Lyot who invented the coronagraph in 1930. The instrument was primarily designed for a permanent observation of the solar corona. But, in 1938, with the proper (Hα) filter and a camera, B. Lyot, could perform the first cinematography of prominences shown at the International Astronomical Union General Assembly in Stockholm in 1938. After his death in 1952, his colleagues built a movie called "Les flammes du Soleil" (or "The flames of the Sun") which demonstrates the variety of structures and their extreme variability (see, e.g., http://www.canal-u.tv/video/cerimes/flammes_du_soleil.9171). In the 1960s, R. Dunn (1960, 1965) used the fine Hα structure of a prominence for measuring the instrumental profile of his instrument (Dunn 1965, Fig. 36, p. 80). He also performed cinematography of prominences which showed that the thin threads or "ropes" (about 300 km across) were the location of downward and also upward vertical motions in the range 5–10 kms^{-1} (Engvold 1976). It is worth mentioning that R. Dunn built the first evacuated solar telescope (the famous solar tower at Sacramento Peak), which solved the issue of the internal telescope seeing and allowed for a spatial resolution below 1 arcsec. In doing so, it contributed much to the study of prominences, along with the solar telescope at Big Bear Solar Observatory and now the New Vacuum Solar Telescope at the Yunnan Observatory (Xu et al. 2014). The vacuum solution was used for the Solar Swedish Telescope (see below) and others but the entrance window was limited to about 1 m. The difficulty is now being overcome with open telescopes such as the Dutch Open Telescope (DOT), the German Gregor Telescope (1.5 m) and the planned ATST (4 m, see below).

For the fine structure (imaging) studies of prominences, the coronagraph remains the main instrumental tool, with the proper filter tuned in a "cool" line appropriate for observing prominences. For instance, since 1994, in support to SOHO, the Pic-du-Midi coronagraph has continuously provided daily images in the Hα line and now in the 1083 nm line of Helium. This program (http://www.climso.fr/index.php/fr/) is run every day by amateurs organized within the "Observateurs Associés" Society. Among the many coronagraphs installed all over the world let us note

the 40 cm coronagraph at the John W. Evans Solar Facility in Sacramento Peak Observatory in the U.S.A., the 52 cm coronagraph at Kislovodsk (then Soviet Union) and now the Large and Small coronagraphs installed in Wroclaw (Poland) and Rhozen (Bulgaria) by Bogdan Rompolt.

1.1.5 A (Relatively) New Technique: Polarimetry for Accessing the Magnetic Field

The connection between prominences and magnetic field was quickly recognized when Babcock and Babcock (1955) noted that filaments mostly coincided with the neutral line between regions with opposite polarities, i.e. the line where the vertical component of the magnetic field is null. This led to the natural question: what is the magnitude and orientation of the magnetic field? The endeavour of its measurement started with observations at the Crimean Solar Tower where H. Zirin (then in sabbatical year) and A. Severny (1961) derived from Zeeman splitting in the Hβ line, magnetic field values of the order of 200 G in an active prominence (and lower values in a quiescent one).

By 1964, an HAO-designed magnetograph was implemented at the HAO Climax Observatory. Systematic measurements were then performed and a more versatile magnetograph was installed by Einar Tandberg-Hanssen (Harvey and Tandberg-Hanssen 1968) which led to two Ph.D. thesis (Rust 1966; Harvey 1969).

In the 1970s, the Hanlé effect, well adapted for the measurement of weak fields, was used through polarimetric observations made at the Pic-du-Midi Observatory (Leroy et al. 1977; Sahal-Bréchot et al. 1977). Details on the techniques and the results are given in Chap. 8 (Lopez Ariste 2014) devoted to the magnetometry of prominences. A new era in the study of prominences opened up thanks to gradually larger instruments collecting more photons with higher polarimetric sensitivities. A next step in this direction will be the 4-m Advanced Technology Solar Telescope (ATST) and its spectropolarimeters (see Sect. 1.2).

1.1.6 Prominences from Space: The Beginnings

Since the very beginning of the solar space era, prominences were systematically observed with all of the advantages linked to space: access to new wavelength windows (especially the UV and EUV), continuity of observations (up to 24 h a day), coupled with gradually better spatial resolution due to progress in the pointing stability. Since the spacecraft were not recovered, the detectors could only be photoelectric devices (photomultipliers, channeltrons, . . .) which had the serious drawback of being monopixel, a major difficulty for building an image! The whole series (one to eight) of Orbiting Solar Observatories and the Solar Maximum

Mission of NASA had to rely upon a method of rastering, i.e. moving the whole instrument and consequently the solar image on the entrance slit of the spectrometer, a motion which could take typically about an hour. In the spectrometer itself, the spectroscopy was performed by rotating a diffraction grating. The spatial resolution was limited by the width and the height of the integrating slit: with a too high slit, the spatial resolution was too poor while with a too short slit, the collected number of photons was too small and the time for scanning an area was too long. The difficulty was (temporarily) overcome with the Skylab mission, when the US astronauts used a dedicated telescope, the Apollo Telescope Mount (ATM), associated with films as detectors, films which were brought back to Earth for processing. Beautiful results were obtained until 1974 through the three visiting periods by the astronauts. Then the Skylab station was put in a sleeping mode and finally desintegrated in the Earth atmosphere, probably because of the high level of solar activity which resulted in an increase in atmospheric drag that affected the orbit of this spacecraft.

Another difficulty was related to data processing, and in particular, the production of representative images by (big) computers on films which were then visualized on dedicated machines comparable to a slide or a film projector in a movie theater.

The latest space images recorded on film in the Lα line by Bonnet et al. (1980) on a rocket flight already gave evidence of a sub-arcsecond fine structure (Fig. 1.8).

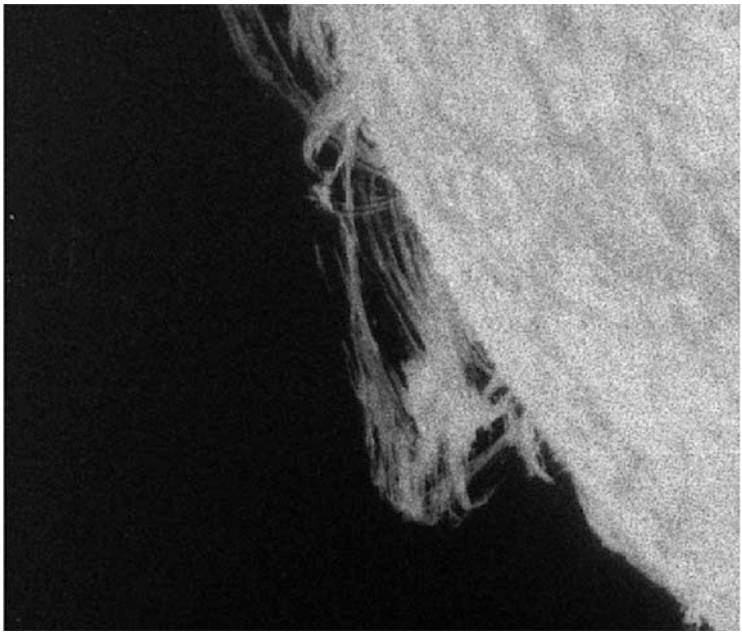

Fig. 1.8 Subimage of a prominence recorded by the Transition Region Camera in the Lα line of hydrogen at 121.6 nm (courtesy R.M. Bonnet)

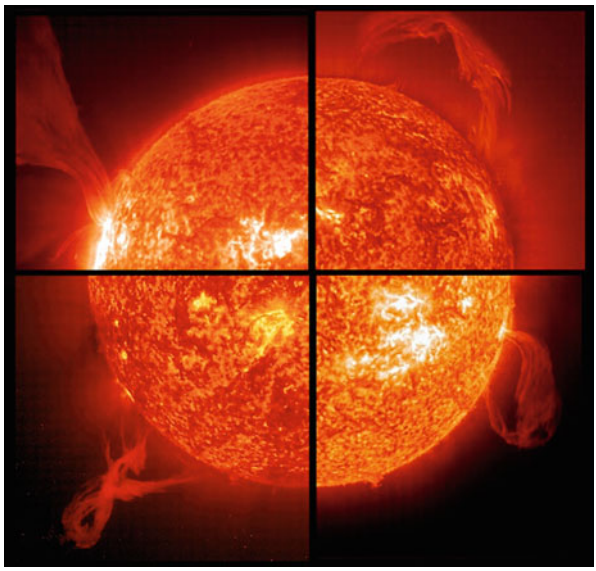

Fig. 1.9 Collage of four Eruptive Prominences caught in action by EIT on SOHO. The observed radiation is the resonance line of He II (singly ionized helium) at 30.4 nm, a line that is formed at about 60,000 K. The images have been obtained in 2000 and 2001 (courtesy, EIT/SOHO consortium)

1.2 The Modern Era

A revolution started in the 1980s with the use of two-dimensional detectors such as CCDs (Charge-Coupled Devices) in astronomy. As with photographic film, it is possible to obtain instantaneous images (at the focus of the telescope or the coronagraph) or spectra at each pixel of the slit (in the focal plane of the spectrograph). This major advance occurred first in ground-based instrumentation and then extended to space where detectors working in the EUV-UV were developed. A beautiful example is provided by the Extreme ultra-violet Imaging Telescope (EIT) on SOHO, which has been observing the Sun (including prominences) since 1996. Since SOHO was positioned around the Lagrangian point L1 between the Sun and Earth, continuous observations became possible; this allowed to catch all dynamic phenomena during their evolution such as eruptive prominences, samples of which are given in Fig. 1.9.

This unique position of SOHO benefited the whole package of instruments (imagers, coronagraphs, spectrographs, magnetograph and in situ experiments) which were extensively used by scientists working on solar prominences.

SOHO detected thousands of Coronal Mass Ejections (CME) (mostly associated with eruptive prominences) which were followed by the EIT imager and then by the LASCO coronagraphs.

But scientists were feeling some frustration because they always viewed these structures only as projected in the plane of sky. The idea of having two viewpoints led to the STEREO mission when two spacecraft at 1 AU separated on October 2006, one being Ahead (A) and the other Behind (B) the Earth. Actually, one has access to a third viewpoint at the Earth orbit, provided by EIT on SOHO and since

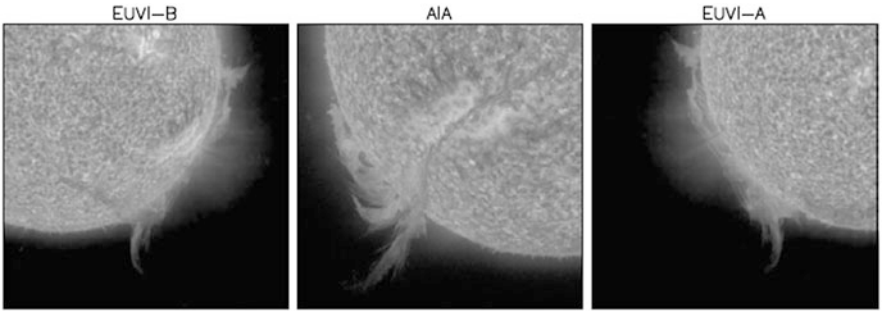

Fig. 1.10 An eruptive prominence observed on December 6, 2010, during its ascent from three different viewpoints by the STEREO A (Ahead) and B (Behind) spacecraft (separated by 172°) and the AIA telescope on SDO in Earth orbit. Note that movies (movie_with_aia.mov and prom_20101206b.mov) are available in the Electronic Supplementary Materials of the paper (from Thompson 2013)

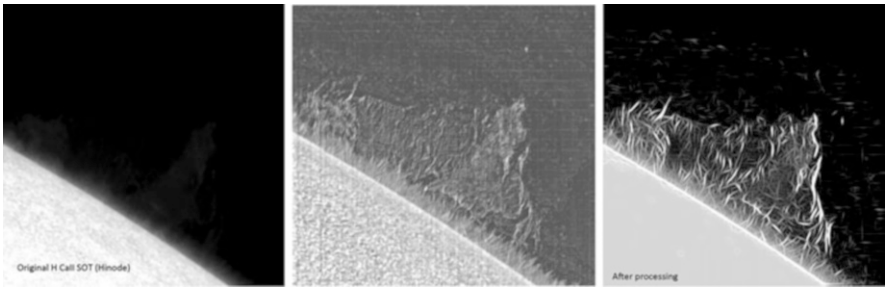

Fig. 1.11 Prominence seen in H Ca II by the Hinode SOT on 22 June 2010 (*left*) and processed by OMC (Octodirectional Maxima of Convexities) (*middle*) and additionally denoised using the 2-D Morlet wavelet (*right*) in order to suppress artefacts and enhance the contrast (from Tavabi et al. 2013)

2010, the AIA telescope of Solar Dynamics Observatory in the same EUV 30.4 nm line (Fig. 1.10).

In the same year, on 23 September 2006, Japan launched the Hinode mission with a set of instruments (Kosugi et al. 2007), one of them being the Solar Optical Telescope with its 50 cm aperture and spectropolarimeters. High resolution images were obtained in the Hα line of hydrogen and the H line of ionized calcium (Fig. 1.11, left).

Major progress has also been made in the field of image processing, as shown in Fig. 1.11 middle and tentatively in Fig. 1.11 right. Actually, image processing is now part of instrumentation as recently demonstrated by a dedicated volume of Solar Physics (2013, Vol. 283/1). For instance, automated detection and tracking of filaments are now routinely performed, an information which ends up in complete databases easy to access through their catalogs (see e.g. Bonnin et al. 2013).

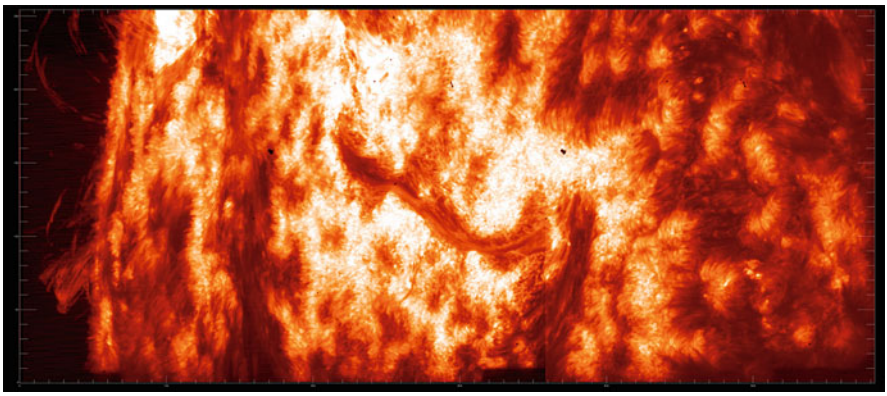

Fig. 1.12 Composite of images recorded by the VAULT rocket experiment in the Lα line of Hydrogen at 121.6 nm. The total field of view is 583 × 234 arcsec (courtesy A. Vourlidas and Vourlidas et al. 2010)

In order to fully appreciate the dynamical behavior of prominences (even the quiescent ones) movies are built and accessible on the www. For instance, one can find a spectacular movie at: http://www.youtube.com/watch?v=l5T1s7Wf5P0 and also the mpeg animation of Fig. 1 of Berger et al. (2008).

As one can see in Fig. 1.11, the field-of-view of the SOT on Hinode is somewhat limited (which allows for its high spatial resolution). The TRACE (Transition Region and Coronal Explorer) satellite also provided a wealth of 8 by 8 arcmin UV and EUV images between 1998 and 2010 from which a huge database was built including filament/prominence movies (http://trace.lmsal.com/POD/bigmovies/filaments/).

The VAULT rocket (Korendyke et al. 2001) also recorded the very fine structure of an active region filament (and prominence) in the Lα line with a 0.4 arcsec resolution but through a set of different exposures with a wider field of view (Vourlidas et al. 2010; Vial et al. 2012). See Fig. 1.12 and compare the fine structure in the prominence with Fig. 1.8.

In order to get a global view of the solar atmosphere (including its prominences), one needs a full-Sun imager providing information about different levels in the atmosphere, corresponding to different lines and consequently temperatures. In order to have a continuous view at high temporal resolution, one needs the proper orbit and a very high telemetry rate. These are the main features of the NASA Solar Dynamics Observatory, launched on February 11, 2010. Being in a geosynchronous orbit, it can look at the Sun permanently and it can transmit science data to the station below at the amazing rate of 130 Mbps. One of the imagers (AIA for Atmospheric Imaging Assembly) working in the He II line at 30.4 nm (see Fig. 1.13), can provide an image of prominences and filaments on the disk every 12 s, 24 h a day! With such a cadence, many movies show spectacular prominence eruptions on the basis of images such as the one of Fig. 1.13 (Movies can be found at: http://sdo.gsfc.nasa.gov/gallery/main). In the framework of SDO observing plans

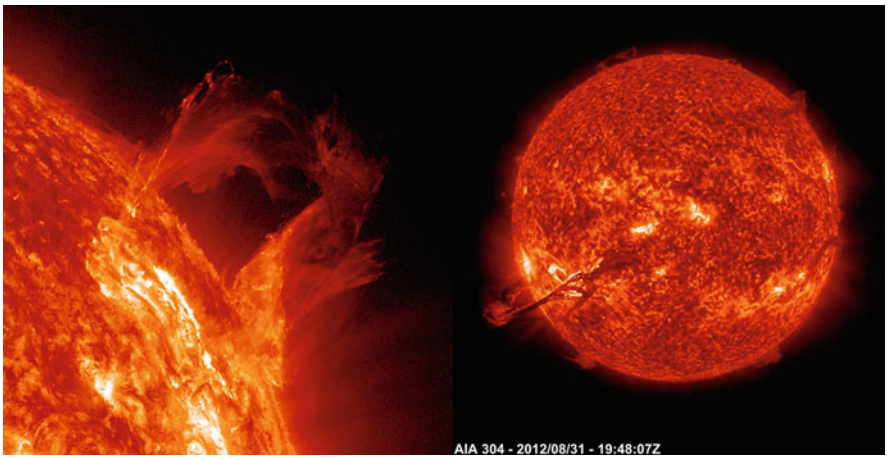

Fig. 1.13 *Left*: Prominence eruption on March 16, 2013, in the He II 30.4 nm line, as viewed by AIA on SDO. *Right*: Prominence eruption following a C-class flare as seen by AIA/SDO in the He II line at 30.4 nm. Note bright and dark regions of the prominence depending on their orientations, the bright ones being illuminated by the solar chromosphere and the dark ones being shielded by the prominence material. Also note that filaments are clearly visible as dark features on the disk in this EUV line (Courtesy AIA/SDO)

and database, catalogs of filaments and prominences have been built for a systematic detection of eruptions (see e.g. http://www.helioviewer.org/ where one can find catalogs of filaments, filament activations and filament eruptions).

Space instrumentation is limited to (relatively) small apertures, the SOT and its 50 cm being an exception. On the ground, most telescopes are, as we shall see, in the 1 m-class. Such large apertures allow for a better spatial resolution (if the distortions by the Earth atmosphere are properly corrected) or a higher photons collecting power (very useful for spectroscopy and polarimetry which are photon-starved).

We give a few examples of ground-based instrumentation below.

Recent improvements in ground-based observatories include speckle processing which is currently performed at the Dutch Open Telescope (DOT) in Canary Islands (Fig. 1.14). The peculiarity of this telescope of 45 cm aperture is that it is open to the wind which homogenises the air temperature and provides better seeing. Through despeckling (performed post-observation) it can reach a spatial resolution of 0.3 arcsec (Fig. 1.15).

The major revolution was the introduction of adaptive optics (AO) which corrects in real-time the image distortion from the Earth atmosphere. This solution has been used for decades by night-time astronomers but it was a challenge to make it work in solar astronomy because of the large number of low-contrast features. An innovative solution has been implemented at the end of the 1990s at the Dunn Solar Telescope at Sacramento Peak (USA) (see e.g. Rimmele 2000).

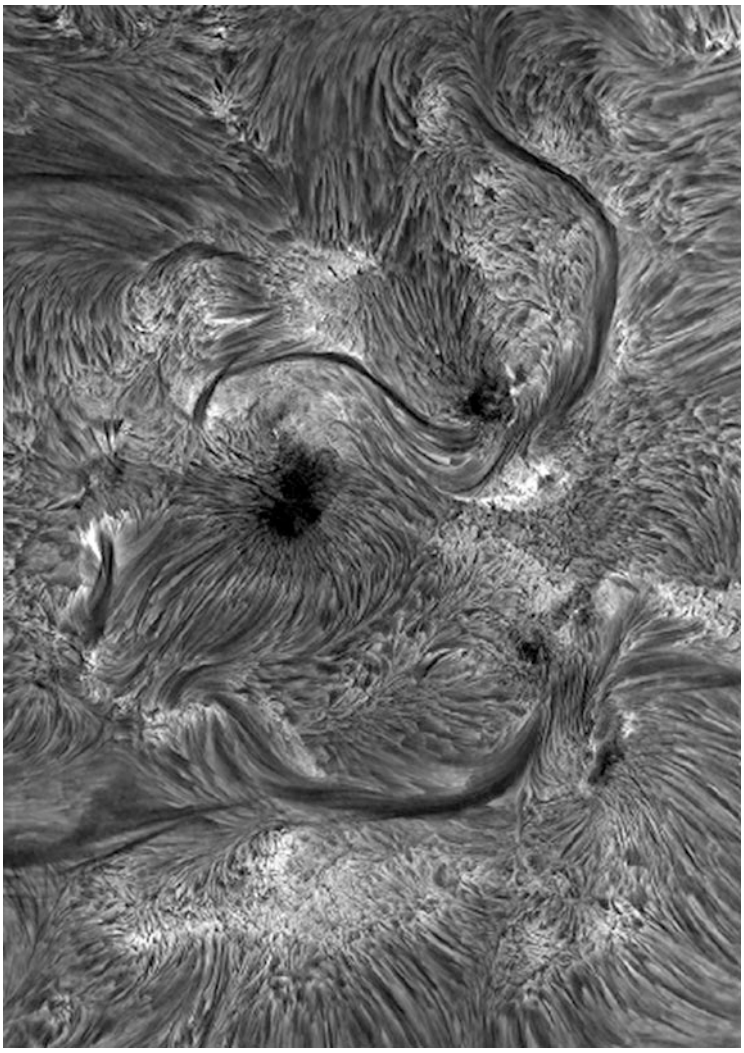

Fig. 1.14 Solar active region AR10786 in an image mosaic obtained by P. Sütterlin with the Dutch Open Telescope on July 8, 2005. The field of view measures 133 × 182 arcsec. The sunspot umbrae remain dark in Hα. The long slender dark structures are active region filaments (courtesy R. Rutten)

This technique is now currently used by the 1-m Swedish Solar Telescope (SST) also operating in the Canary Islands (Fig. 1.16) and the 1.6 m New Solar Telescope at Big Bear. The SST is in addition set up for the application of a post-processing technique called Multi-Frame Blind Deconvolution, enabling diffraction-limited observations (about 70 km) (Scharmer et al. 2003; van Noort et al. 2005).

Fig. 1.15 The Dutch Open Telescope (DOT) with its canopy closed

An example is given in Fig. 1.17 where one can see quasi linear threads probably tracing the magnetic field in a special part called a "barb" found sticking out from the main body of filaments (Lin et al. 2005).

Imagery, even performed simultaneously in different wavelengths, allows us to trace the apparent motions of the prominence but it does not provide an as precise plasma diagnostics as spectroscopy which also adds information on plasma motions along the line-of-sight. Major advances in spectroscopic instrumentation have been obtained with the Extreme Ultraviolet Imaging Spectrometer (EIS) on Hinode (Culhane et al. 2007), a spectrograph which focused on EUV coronal lines but could record the Lβ line of He II at 25.6 nm in prominences.

Fig. 1.16 Swedish 1-m Solar Telescope (SST) in Canary Islands

Another major step was recently obtained with the Interface Region Imaging Spectrograph (IRIS) which was launched on June 27, 2013 by a Pegasus rocket from an Orbital L-1011 aircraft. It is a spectrograph working in the UV (140 nm) and Near UV (280 nm) fed by a 20 cm telescope (Fig. 1.18).

This aperture and the pointing stability allow for a spatial resolution close to 300 km on the Sun. The orbit being heliosynchronous, it is possible to observe the Sun continuously all the year round (except for some eclipses from November to February). Actually, imaging is possible on IRIS in two different ways:

1. through motion of the entrance slit (called raster mode) which provides the full spectrum at each spatial position,
2. through a permanent solar image at the (reflecting) "jaws" of the slit (called slit-jaw imaging). This latest device is well-known by ground-based observers who usually rely upon an Hα image. Its implementation on IRIS has the peculiarity of recording the image in UV lines, which provide the right context for UV spectra.

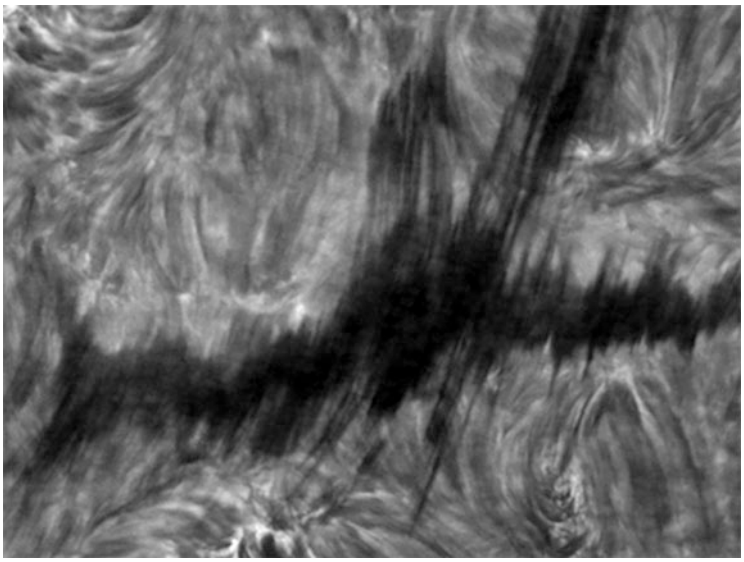

Fig. 1.17 Hα picture of the "barb" of a filament taken with the SST (courtesy O. Engvold)

Fig. 1.18 A view of the IRIS instrument (telescope and spectrograph) mounted on the S/C. Note the guide telescope on top of the telescope (courtesy A. Title)

The combination of slit-jaw images and spectra at high cadence allows the construction of spectacular movies available at: http://www.lmsal.com/hek/hcr?cmd=view-recent-events&instrument=iris.

The UV channel records spectral lines such as the resonance lines of Si IV and C IV formed in the Prominence Corona Transition Region (PCTR), at temperatures of a few 10,000 K (see Chap. 3, Parenti 2014). The NUV channel focuses upon an interesting doublet of Mg II: the "h" (280.271 nm) and "k" (279.553 nm) lines named by analogy with the H and K lines of Ca II. Similarly, they are formed at temperatures lower than 15,000 K in the cool core of prominences. Figure 1.19 provides an example of Mg II h and k spectra obtained at the South Pole of the Sun.

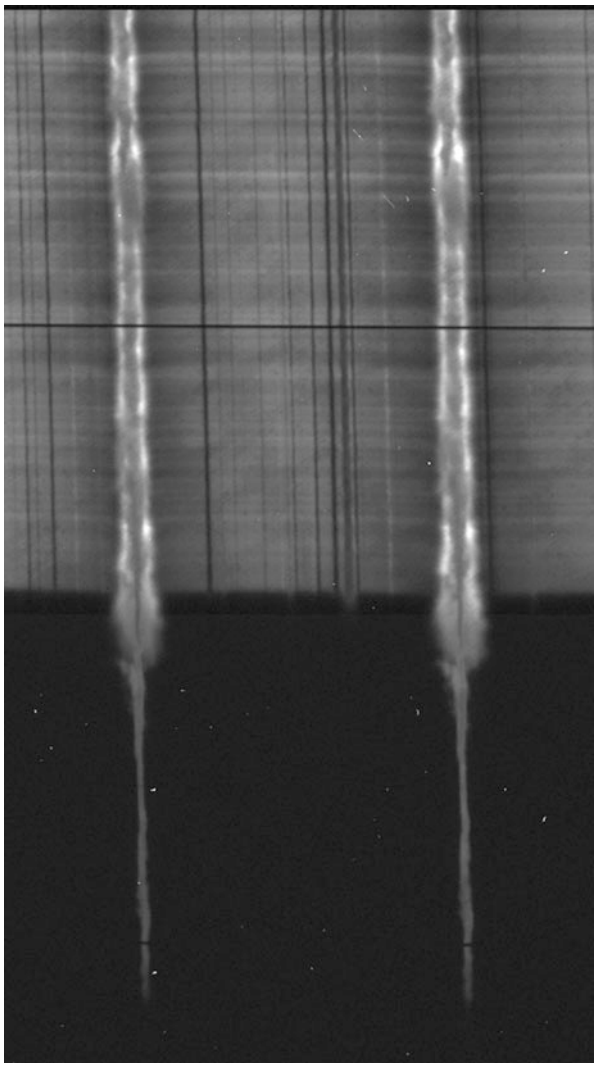

Fig. 1.19 Uncalibrated stigmatic spectra of the Mg II k and h lines observed by IRIS. The lower part of the figure where the profiles are narrow corresponds to a prominence of the polar crown seen above the South Pole limb. The upper part of the figure where profiles are wide and reversed corresponds to the chromosphere close to (and just above) the limb (courtesy A. Title—LMSAL) (see also Fig. 1 of Heinzel et al. 2014)

Note the very narrow unreversed profiles in the prominence, which correspond to very thin threads as shown in Chaps. 2 and 6 (Engvold 2014; Labrosse 2014).

Actually, the slit-jaw observing mode has the advantage of providing a context but has the drawback of ignoring the spectral profiles outside the slit. In the case of IRIS, one can also move the image on the slit, a mode which provides instantaneous spectra. Other modes are possible, on the ground and in space, where one records simultaneous spectra and simultaneous monochromatic images.

This is currently done with a dual Fabry-Perot in the Interferometric BIdimensional Spectrometer (IBIS), or the Universal Birefringent Filter at the Dunn Solar Telescope of Sacramento Peak. These devices have allowed a tremendous progress

Fig. 1.20 THEMIS (Heliographic Telescope for the Study of the Magnetism and Instabilities on the Sun) in Canary Islands

not only in the recording of broad chromospheric lines but also prominence/filament line profiles because they allow for a rather easy derivation of the line-of-sight velocities through the comparison of "blue" and "red" parts of the lines. Another original scheme consists in a multichannel substractive double-pass spectro-imaging (MSDP) which is a grating spectrometer providing simultaneous images (with a typical field-of-view of 30 by 250 arcsec) in nine bands in the selected line (e.g. Hα). It has been implemented in various observatories including the 90-cm aperture THEMIS (Heliographic Telescope for the Study of the Magnetism and Instabilities on the Sun) in Canary Islands (Fig. 1.20).

Let us also mention the powerful CRisp Imaging SpectroPolarimeter (CRISP) of the SST (first described by Scharmer 2006). It provides 2-D monochromatic images in more than ten wavelength positions in a line such as H-alpha in the course of a very few seconds.

A major project, now under construction in Hawaï, is the Advanced Technology Solar Telescope (ATST now named Daniel K. Inouye Solar Telescope) built by the National Solar Observatory in the U.S.A. Its primary mirror is an off-axis paraboloid with a 4.24 m diameter (limited to a 4-m aperture) which will be the first monolithic solar mirror of this size ever built. The heat stop assembly will define a field of view of 5 by 5 arcmin. The secondary is a 65 cm off-axis aspheric concave mirror, in SiC, a material with excellent thermal and physical properties. A very useful device for coronagraphic observations (including prominences, Rimmele et al. 2014) is a Lyot stop located at the first pupil image. ATST benefits from adaptive and active optics system at its Coudé focus (the Multi Conjugate Adaptive Optics, a tool used to extend the field of view, see e.g. Langlois et al. 2013) and will provide a spatial resolution eight times better than the SOT on Hinode. The following instrumentation is a complex set of imagers and spectropolarimeters (see Fig. 1.21). ATST is expected to see its first light in 2019. (Note that Europe also has a 4-m

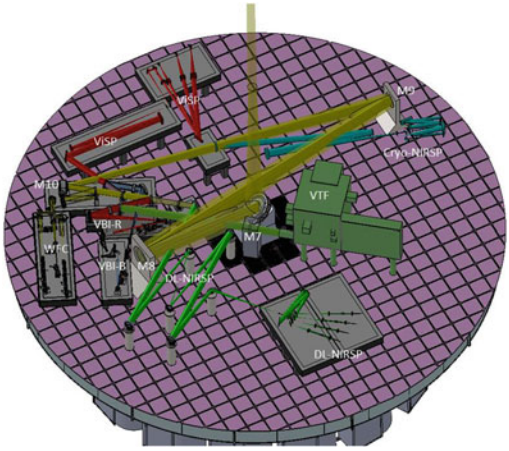

Fig. 1.21 ATST instrumentation at the Coudé level. It includes a Visible Broad-band Imager, a Visible Spectro-Polarimeter, two Near-IR Spectro-Polarimeters, and a Visible Tunable Filter (see http://atst.nso.edu) (courtesy of NSF/AURA/NSO/DKIST)

telescope project EST: see http://www.est-east.eu/, India proposes a 2-m National Large Solar Telescope and China has plans for a 6–8 m Giant Solar Telescope).

At that time, the Solar Orbiter mission of ESA (and NASA) and the Solar Probe Plus of NASA, will have started their journeys close to the Sun and other S/C from Russia, Japan (and other Agencies) will be monitoring the Sun. It will then be essential to coordinate the observations from these space and ground-based instruments as has been done in the past. With the SOHO mission, periodic campaigns based on Joint Observing Programs included SOHO, TRACE and many ground-based observatories. This allowed coverage of a large range of wavelengths and to perform a multi-temperature analysis. The joint analysis was facilitated by the use of common FITS formats and software such as SolarSoft (http://www.lmsal.com/solarsoft/). The same procedures were used for Hinode which was operated from Japan.

1.3 The Rich Physics Associated with Prominences

As the reader will see throughout the book, prominences provide an amazingly large playground for different fields of physics. The very fact that they exist as cool and dense structures in the hot and diffuse coronal "furnace" is a challenge for plasma physicists. Although downward motions are observed, why does the material not drop in free fall, as already noticed by Rothschild et al. (1955)? The challenge is increased since their gas (or plasma) is far from being totally ionized, which means that many plasma processes can occur which can lead to instabilities (plasma gradient, Rayleigh-Taylor, MHD wave damping, ambipolar diffusion). Since, as will be seen later on, the density and more importantly the magnetic field are still not precisely determined, it is not clear how much the magnetic pressure dominates the kinetic pressure. The ionization also depends on the proximity of an active

region (or a flare) with a strong ionizing radiation field. Since the early works of Kippenhahn and Schlüter (1957) and Kuperus and Raadu (1974) more and more complex magnetic models have been built. The structuring in very thin threads is also an enigma increased by our ignorance of the actual size of these threads. In view of the large diversity of these structures (already noticed by early observers), along with their temporal variability, it is not possible to build detailed realistic models, even empirical. But progress has been made towards a description of prominences with a set of slender cylinders and loops, as we shall see in the book. Apparent flows and intensity variations are still discussed in about the same terms as by Secchi (see Sect. 1.1.2): are they actual (fast) mass transports or simply local variations of the excitation of a permanent plasma? Moreover, it has been demonstrated by Rompolt (1980) that radial flows may strongly affect line emissivity.

Since determination of the physical conditions in these structures relies upon remote sensing observations, this requires also the understanding of the radiative processes in relation with the plasma properties. And it just happens that prominences are strongly out of (local) thermodynamic equilibrium from the standpoints of populations of atoms and ions and consequently of the emitted radiation. In some lines, the plasma is optically thick, which complicates the diagnostics. Another basic fact which still is not understood is the heating of prominences. This can be seen as a paradox since the prominence plasma is much cooler than the surrounding corona. But in terms of radiative equilibrium (e.g. in the Lyman continuum) prominences should be cooler than observed (Heasley and Mihalas 1976; Fontenla 1979), which implies a heating process still unidentified in spite of many candidates (Alfvèn waves energy deposit, ambipolar diffusion, . . .).

The very existence of prominences is still not well understood. The understanding of their formation, their stability and their eruption requires a great deal of information about the plasma and the magnetic field, inside, beneath and around the structures. This requires a comprehensive set of multi-wavelength observations requiring the best spectral, spatial and temporal resolutions that are often impossible to perform. MHD modelers and theoreticians have to live with this incomplete information that they circumvent by clever schemes such as field extrapolation. The very fact that prominences are dynamic also increases the difficulty of their task.

In summary, the study of prominences calls for an interdisciplinary approach involving various techniques (imaging, spectroscopy, polarimetry), matter-radiation interaction physics, plasma physics, etc. This approach is the essence of the book.

1.4 The Aim of the Book and to Whom It Is Addressed

Since the publication in 1995 of the latest book devoted to solar prominences ("The nature of solar prominences" by Einar Tandberg-Hanssen (1995), Kluwer) very important new results have been obtained from space missions and ground-based observatories. During more than 18 years, SOHO has provided 24 h a day continuous observations of the Sun in general and prominences in particular. SOHO

was complemented by the high spatial resolution TRACE. The STEREO mission has provided two viewpoints allowing for a stereoscopic view of the Sun... and prominences. The Hinode mission offered a unique opportunity of studying the fine structure of prominences. More recently, the Solar Dynamics Observatory (SDO) has provided continuous high-cadence sets of spectacular images from which movies have been built, now available on the internet. In 2013, the UV spectro-imager IRIS (Interface Region Imaging Spectrograph) was launched and since then has observed prominences. On the ground, the new Swedish Solar Telescope (SST) and the Dutch Open Telescope (DOT) have recently provided unique images of prominences and filaments. Consequently, the ambition of the book is to present a comprehensive and pedagogical approach of prominences based upon the latest results obtained by the most recent instrumentation along with the up-to-date theories and modelling.

The book is intended for advanced students in astrophysics, post-graduates, solar physicists and more generally astrophysicists. Being based on many spectacular images, it can also be useful for amateur astronomers interested in this enigmatic feature of our fascinating Sun.

1.5 Table of Contents of the Book

After the present general introduction, Chap. 2 describes prominences in detail, their structures and their environment and discusses the various classifications, a difficult task when one considers the variety and the temporal variation of structures that we have seen in this Introduction. In this chapter, we alternately zoom in on the fine structure and zoom out on the large-scale features. Among these, the large-scale spine (which follows the Polarity Inversion Line) and the small-scale barbs (which connect to the chromosphere) are presented.

Once prominences are well identified, Chaps. 3–7 present their thermodynamic properties along with the ingenuous methods used to derive them.

Chapter 3 is devoted to the spectral diagnostic of optically thin plasma, in the cool core and in the hotter Prominence-Corona Transition Region (PCTR). Although the methods used seem to be "simple", the results (e.g. the "Hvar model" see Engvold et al. 1990 and also Patsourakos and Vial 2002) largely depend on the observed structures and in particular their sizes limited by the spatial resolution of the observation. However, the results derived from the latest missions put more constraints on the temperature, the neutral and electron densities, ionization degree and other thermodynamic quantities.

Chapter 4 covers the issues of the derivation of mass and velocity flows allowing determination of mass flows. These physical quantities are the key to understanding the mass and energy equilibria and consequently the stability of prominences. The presentation of the methods used leads to the uncertainties in the mass and flows which are derived. Moreover, the orientation and the magnitude of the flows largely depend on the observed structures (e.g. spine and barbs). Among some outstanding

issues, the chapter discusses the origin of mass flows, the possible role of barbs, the relation with cavities (see Chap. 13) and with the magnetic structuring.

Chapter 5 is an introductory tutorial on radiative transfer and Non-Local Thermodynamic Equilibrium (NLTE) forward modelling, whether in one or two dimensions. This tutorial is focused on the specific case of prominences i.e. structures illuminated from below (photospheric and chromospheric radiation) and from all around (EUV coronal radiation) which moreover can be submitted to a changing Doppler-shifted illumination depending on their motion. It addresses the specific case of radiative transfer in radio wavelengths. It presents new techniques for coupling radiation and magneto-hydrostatics. It allows to better understand the following Chap. 6 which presents the results of the NLTE modelling and compares them to observations. Note that this chapter also addresses the prominence radio emission.

Chapter 6 presents the (direct) method used for deriving the major properties of prominences through non-LTE modeling. It shows that the direct method is both necessary and difficult because of the complex coupling between radiation and plasma. No thermodynamic quantity can be easily derived from the spectroscopic observation of optically thick lines (and continua). But some laws between observed radiation and emitting plasma can be derived as a result of systematic modeling. The chapter shows how major progresses have been made when moving from one-dimensional (1D) "monolithic" models to a set of 1D slabs simulating a bunch of threads and when comparing with 2D models. The modeling concerns basically the hydrogen and helium elements (which determine the ionization ratio) but also the "trace" elements (e.g. Ca II, Mg II) which provide still more constraints.

Chapter 7 addresses the fundamental issue of stability of prominences with a thorough description of all the terms entering the energy equation. These terms have been derived and discussed in the case of the chromosphere and the chromosphere–corona transition region. The basic approach consists in establishing the list of all possible losses and to derive the required energy input. Essentially two regions are considered: a cool core (less than 10^4 K) and a prominence–corona transition region (PCTR) (from 10^4 to 10^6 K). The conductive flux is negative in the PCTR and positive in the cool core. The enthalpy flux is important in the PCTR as a heating process, along with the radiative losses which peak at a few 10^4 K at constant pressure. Other heating mechanisms (waves, ...) are also considered. Finally, Chapter 7 discusses the energy balance of quiescent prominences (cool core and PCTR) and the various models which satisfy the observational constraints.

Chapters 8–13 introduce a very important and recently studied ingredient, the magnetic field coupled with the dynamics of prominences.

With Chap. 8, we are introduced to the techniques and the results of prominence magnetometry and its forward and inverse solutions. Actually it is a tutorial on the two main modifications of the radiation polarization induced by the presence of magnetic fields. Zeeman and Hanle effects are described and compared in the context of prominences. It is shown that the Hanle effect is the main tool and that old Zeeman measurements provided values of the magnetic field which were, by chance, not far from the actual ones. In the case of the forward problem, the scattering

is treated rigorously for the He lines for both linear and circular polarization. The techniques related to the inverse (mathematically ill-posed) problem are also presented. This chapter ends with a critical discussion about the ambiguities, sources of error and uncertainties in prominences magnetometry. It also proposes paths for improving the field derivation such as inclusion of radiative transfer, 3D geometry, etc.

Chapter 9 covers the issue of the magnetic field structure, as derived from direct and indirect observations. It provides the detailed specific characteristics of the two main types of prominences (channel and coronal clouds) prominences. As far as channel filaments are concerned, they are essentially defined by the presence of a polarity reversal boundary as revealed by magnetograms. The usual three classes (active region filaments, intermediate and quiescent filaments) are precisely defined and their magnetic properties derived, one would dare to say surprisingly, from patient temporal sequences of spectroheliograms. Amazing pictures at high spatial resolution are complemented by labels which provide support to the text. The chapter also puts the emphasis on a new physical quantity: the chirality. Overall the reader will have access to a complete and consistent picture on the essential rôle of the magnetic field in structuring, stabilizing and destabilizing prominences at all scales.

Chapter 10 covers the dynamics (models and observations) related to the formation of prominences. It provides some answers to the important question: where does the material come from? from the "sky" above or from the "ground" below? It recalls the many observational constraints imposed by observations such as the observed flows (and their directions). Then it reviews the four main models of mass formation: injection (from the chromosphere), levitation (by the magnetic field), evaporation-condensation (by which the plasma is heated and then cooled by radiative losses) and magneto-thermal (based on Kelvin–Helmholtz instability) models which are discussed in terms of observational signatures. The review comes with dedicated didactic cartoons and, where necessary, the presentation of basic physical processes such as magnetic reconnection.

In Chap. 11, some basics of MHD waves are introduced and the properties of MHD waves fully described. The different modes of oscillations are discussed in two different geometries: slabs and threads. The comparison of observed oscillation periods and damping times with the predicted values offers a new diagnostic tool: prominence seismology. This analysis has been recently improved (and complexified) with the inclusion of flows in the geometrical models and the coupling of MHD waves and radiative transfer (also see Chap. 5). Obviously, the determination of plasma parameters and the precise geometry of the prominence would be benefitting for the seismology (e.g. derivation of the magnetic field) and reciprocally.

Chapter 12 focuses on the MHD simulations of the emergence of twisted magnetic flux tubes which can ultimately lead to prominence eruption through build-up of free energy and helicity in the corona. It distinguishes between ideal MHD instabilities (essentially torus and kink instabilities which are treated both analytically and with numerical simulations) and fast magnetic reconnection in current

sheets. Many modeling results are convincingly compared with observations. The issue of the hypothesis of force-free coronal structures is also discussed.

Chapter 13 focuses on coronal cavities whose importance has been stressed with the new Hinode (SOT) observations along with MHD models. The difficulty of observing cavities should not conceal the fact that they are probably ubiquitous. Their location, morphology and thermal properties are thoroughly presented, along with plane-of-sky and line-of-sight flows. For each observation, a MHD model is proposed. Polarimetry puts forward an essential ingredient: the magnetic field parallel to the underlying neutral line. Cavities are shown to be dependable predictors of prominence eruption. The whole chapter leads to the conclusion that cavities actually are magnetic flux ropes.

Chapter 14 describes large patterns and filament channels taking into account the large number of filaments/prominences and their evolution over time spans of the order of a solar rotation (and more). The chapter is based upon the three categories defined in Chap. 2: quiescent filaments (QF), intermediate filaments (IF) and active region filaments (ARF). It first focuses on the formation locations which most often involve multiple bipole interactions. The chirality follows an hemispheric pattern with some exceptions. From patient (but not so numerous) observations, it is possible to distinguish two mechanisms at work: reconfiguration of pre-existing coronal fields vs. emergence of horizontal flux tubes. The chapter provides an extensive list of models which can explain the observations and concludes on the statement that different mechanisms can be at work for the three classes of prominences.

Chapters 15–17 pay attention to the final phase of prominence eruptions (PE) and their impacts on Earth.

The dynamics of eruptive prominences (EP), up to 1 A.U. are detailed in Chap. 15. It is shown that EPs cannot be separated from flares and Coronal Mass Ejections (CMEs), as evidenced by statistical associations, correlated cycle variations and joint kinematics. The (cool) ejected material can be followed far in the heliosphere with such in situ signatures as low-charge Fe ions or increased He^{+}/He^{++} ratio. Attention is paid to high-latitude prominences whose "rush to the pole" and further eruption play role in the polarity sign reversal at the poles. The chapter also shows that polar CMEs are similar to low-latitude CMEs, an indication of a common bipolar origin. Finally the non-radial motions of EPs and CMEs are compared, an important issue in the frame of Space Weather.

Chapter 16 is also devoted to the relation between Eruptive Prominences and Coronal Mass Ejections from the point of view of CMEs, with focus on detailed observations (and properties) of EPs rather far in the heliosphere through remote-sensing techniques. The three-component classical model of CMEs is presented with the (new) evidence of the presence of a flux rope. Respective mass and energy values are discussed. Farther in the interplanetary space, it is more and more difficult to identify the EP cool material with remote-sensing. However, apart from in situ detection of magnetic clouds, it has been recently made possible to identify EP with the help of Heliospheric Imagers (HIs) on board STEREO and SMEI missions.

Chapter 17 further details the propagations of EPs and CMEs in the interplanetary medium with the help of the unique HI observations on STEREO. The simulations which take into account the (magnetic) interaction with the solar wind confirm the increase of mass, by a 2–3 factor, up to 1 AU. The chapter then focuses on the different impacts of EPs and CMEs on our Earth as measured in situ. It discusses the three mains sources of Space Weather: radiation (EUV, X-ray), high-energy particles accelerated in the interplanetary medium and high-energy particles accelerated inside Earth's magnetosphere. As a conclusion, the Chapter raises the issue of the difficulty of detecting EP material at 1 AU on one hand, and the rôle this cool material could play in CME geo-effectiveness on the other hand.

Chapter 18 opens a new window into non-solar astronomy: stellar prominences and stellar CMEs along with their influence on planetary evolution. Firstly, the chapter reviews some major features of stellar activity. Then it presents the major properties of the more than one thousand exoplanets detected to this day. It introduces the new concept of habitability summarized in a mass/orbit diagram. Because of the impact of stellar radiation and plasma flows on planetary atmospheres, the stellar activity is thoroughly discussed for late-type stars in terms of luminosity, wind and CMEs. The importance of exoplanets magnetic fields is not ignored, even if they cannot be measured! Scaling laws between the exoplanet magnetic dipole, the rotation rate and the radius of the dynamo region are proposed. The chapter derives a value of the minimum magnetospheric radius which provides an effective shielding of the planet. Hot Jupiters are also detailed. As the reader will discover, the issue of prominences on our near Sun naturally leads to the issue of the possibility of life on planets located many light-years away from us.

Acknowledgments I thank O. Engvold, S. Koutchmy and J.W. Leibacher for kindly providing useful material and helpful suggestions and corrections.

References

Babcock, H. D., & Babcock, H. W. (1955). The sun's magnetic field, 1952–1954. *The Astrophysical Journal, 121*, 3.

Berger, T. E., Shine, R. A., Slater, G. L., Tarbell, T. D., Title, A. M., Okamoto, T. J., Ichimoto, K., Katsukawa, Y., Suematsu, Y., Tsuneta, S., Lites, B. W., & Shimizu, T. (2008). Hinode SOT observations of solar quiescent prominence dynamics. *The Astrophysical Journal, 676*(1), L89–L92.

Bonnet, R. M., Decaudin, M., Bruner, E. C., Jr., Acton, L. W., & Brown, W. A. (1980). High-resolution Lyman-alpha filtergrams of the sun. *Astrophysical Journal, Part 2 – Letters to the Editor, 237*, L47–L50.

Bonnin, X., Aboudarham, J., Fuller, N., Csillaghy, A., & Bentley, R. (2013). Automation of the filament tracking in the framework of the HELIO project. *Solar Physics, 283*, 49.

Culhane, J. L., et al. (2007). The EUV imaging spectrometer for Hinode. *Solar Physics, 243*, 19.

D'Azambuja, L., & D'Azambuja, M. (1948). Etude d'ensemble des protubérances solaires et de leur évolution, Annales de l'Observatoire de Paris, Tome VI, Gauthiers-Villars.

Deslandres, H. (1910). Ann. Obs. Paris-Meudon 4 (III), pp. 54–55.

Dunn, R. (1960). Photometry of the solar chromosphere, Ph.D. Thesis, Harvard University.

Dunn, R. (1965). Sacramento Peak Obs. Contr. Report #87, Fig. 36, p. 80.
Engvold, O. (1976). The fine structure of prominences. I – Observations – H-alpha filtergrams. *Solar Physics, 49*, 283.
Engvold, O. (2014). Description and classification of prominences. In J.-C. Vial, & O. Engvold (Eds.), *Solar prominences, ASSL* (Vol. 415, pp. 31–60). Springer.
Engvold, O., Hirayama, T., Leroy, J.-L., Priest, E. R., & Tandberg-Hanssen, E. (1990). Hvar reference atmosphere of quiescent prominences. In V. Ruzdjak & E. Tandberg-Hanssen (Eds.), *Dynamics of quiescent prominences. Proceedings of I.A.U. Colloquium #117, held in Hvar, SR Croatia, Yugoslavia, September 25–29, 1989*. New York: Springer-Verlag.
Fontenla, J. M. (1979). A prominence model based on spectral observations. *Solar Physics, 64*, 177.
Hale, G.E., & Ellerman, F. (1903). Publ. Yerkes Obs. 3(I), 3.
Harvey, J.W. (1969). *Magnetic fields associated with solar active-region prominence.* Ph.D. Thesis, University of Colorado.
Harvey, J., & Tandberg-Hanssen, E. (1968). The magnetic field in some prominences measured with the He I, 5876 Å line. *Solar Physics, 3*, 316.
Heasley, J. N., & Mihalas, D. (1976). Structure and spectrum of quiescent prominences – energy balance and hydrogen spectrum. *Astrophysical Journal, 205*, 273.
Heinzel, P., Vial, J.-C., & Anzer, U. (2014). On the formation of Mg II h and K lines in solar prominences. *Astronomy and Astrophysics, 564*, 132.
Khangil'Din, U. V. (1964). Characteristics of solar active regions obtained from observations on millimeter wavelengths. *Soviet Astronomy, 8*, 234.
Kippenhahn, R., & Schlüter, A. (1957). Eine Theorie der solaren Filamente. Mit 7 Textabbildungen. *Zeitschrift fur Astrophysik, 43*, 36.
Korendyke, C. M., Vourlidas, A., Cook, J. W., Dere, K. P., Howard, R. A., Morrill, J. S., Moses, J. D., Moulton, N. E., & Socker, D. G. (2001). High-resolution imaging of the upper solar chromosphere: First light performance of the very-high-resolution advanced ultraviolet telescope. *Solar Physics, 200*, 63–73.
Kosugi, T., et al. (2007). The Hinode (solar-B) mission: An overview. *Solar Physics, 243*, 3.
Kuperus, M., & Raadu, M. A. (1974). The support of prominences formed in neutral sheets. *Astronomy and Astrophysics, 31*, 189.
Labrosse, N. (2014). Derivation of the major properties of prominences using non-LTE modeling. In J.-C. Vial & O. Engvold (Eds.), *Solar prominences, ASSL* (Vol. 415, pp. 129–153). Springer.
Langlois, M., Moretto, G., Béchet, C., Montilla, I., Tallon, M., Goode, P., Gorceix, N., & Shumko, S. (2013). Concept for solar multi-conjugate adaptive optics at big bear observatory. In S. Esposito & L. Fini (Eds.), *Proceedings of the third AO4ELT conference*. Firenze, Italy, May 26–31, 2013. Online at http://ao4elt3.sciencesconf.org/, id. #62.
Leroy, J.-L., Ratier, G., & Bommier, V. (1977). The polarization of the D3 emission line in prominences. *Astronomy and Astrophysics, 54*, 811.
Lin, Y., Engvold, O., Rouppe van der Voort, L. H. M., & Wiik, J. E. (2005). Thin threads of solar filaments. *Solar Physics, 226*, 239–254.
Lopez Ariste, A. (2014). Magnetometry of prominences. In J.-C. Vial & O. Engvold (Eds.), *Solar prominences, ASSL* (Vol. 415, pp. 177–202). Springer.
Parenti, S. (2014). Spectral diagnostics of cool prominence and PCTR optically thin plasmas. In J.-C. Vial & O. Engvold (Eds.), *Solar prominences, ASSL* (Vol. 415, pp. 61–76). Springer.
Patsourakos, S., & Vial, J.-C. (2002). SOHO contribution to prominence science. *Solar Physics, 208*, 253.
Rayet, G. (1869). Report of M. Rayet. *Astronomical Register, 7*, 133–134.
Rimmele, T. R. (2000). Solar adaptive optics. In P. L. Wizinowich (Ed.), *Adaptive Optical Systems Technology, Proceedings of SPIE* (pp. 218–231).
Rimmele, T., Berger, T., Casini, R., Elmore, D., Kuhn, J., Lin, H., Schmidt, W., & Wöger, F. (2014). Prominence science with ATST instrumentation. In *Nature of prominences and their role in space weather, proceedings of the International Astronomical Union (IAU) symposium* (Vol. 300, pp. 362–369).

Rompolt, B. (1980). Doppler brightening effect in H-alpha line for optically thin moving prominences. *Hvar Observatory Bulletin, 4*(1), 39.

Rothschild, K., Pecker, J.-C., & Roberts, W. O. (1955). The prominence of July 25, 1951. *The Astrophysical Journal, 121*, 224.

Rust, D.M. (1966). *Measurements of the magnetic fields in quiescent solar prominences.* Ph.D. Thesis, University of Colorado.

Sahal-Bréchot, S., Bommier, V., & Leroy, J.-L. (1977). The Hanle effect and the determination of magnetic fields in solar prominences. *Astronomy and Astrophysics, 59*, 223.

Scharmer, G. B. (2006). Comments on the optimization of high resolution Fabry-Pérot filtergraphs. *Astronomy and Astrophysics, 447*, 1111.

Scharmer, G. B., Bjelksjo, K., Korhonen, T. K., Lindberg, B., & Petterson, B. (2003). The 1-meter Swedish solar telescope. In S. L. Keil & S. V. Avakyan (Eds.), Innovative Telescopes and Instrumentation for Solar Astrophysics, *Proceedings of SPIE* (Vol. 4853, p. 341).

Schmahl, E. J., Bobrowsky, M., & Kundu, M. R. (1981). Observations of solar filaments at 8, 15, 22 and 43 GHz. *Solar Physics, 71*, 311–328.

Tandberg-Hanssen, E. (1974). (Geophysics and astrophysics monographs), *Solar prominences* (Vol. 12). Dordrecht: D. Reidel Publishing Co.

Tandberg-Hanssen, E. (1995). Astrophysics and Space Science Library, *The nature of solar prominences,* (Vol. 199). Dordrecht: Kluwer Academic Publishers.

Tavabi, E., Koutchmy, S., & Ajabshirzadeh, A. (2013). Increasing the fine structure visibility of the Hinode SOT Ca II H filtergrams. *Solar Physics, 283*, 187–194.

Thompson, W. T. (2013). Alternating twist along an erupting prominence. *Solar Physics, 283*, 489–504.

van Noort, J. M., Rouppe van der Voort, L. H. M., & L̈ofdahl, M. G. (2005). Solar image restoration by use of multi-frame blind deconvolution with multiple objects and phase diversity. *Solar Physics, 228*, 191–215.

Vassenius, B. (1733). Observation de l'éclipse totale de Soleil avec demeure, faite à Gothebourg en Suède à 57° 40' 54 le 2 Mai 1733, *Philosophical Transactions of the Royal Society of London, 38*, 134.

Vial, J.-C., Olivier, K., Philippon, A. A., et al. (2012). High spatial resolution VAULT H-Lyα observations and multiwavelength analysis of an active region filament. *Astronomy and Astrophysics, 541*, 108.

Vourlidas, A., Sanchez Andrade-Nu˜no, B., Landi, E., et al. (2010). The structure and dynamics of the upper chromosphere and lower transition region as revealed by the subarcsecond VAULT observations. *Solar Physics, 261*, 53.

Xu, Z., Jin, Z. Y., Xu, F. Y., Liu, Z. (2014). Primary observations of solar filaments using the multi-channel imaging system of the New Vacuum Solar Telescope. In B. Schmieder, J.-M. Malherbe & S. T Wu (Eds.), *Nature of prominences and their role in space weather. Proceedings of the International Astronomical Union*, *IAUSymposium* (Vol. 300, pp. 117–120).

Zirin, H., & Severny, A. B. (1961). Measurement of magnetic fields in solar prominences. *Observatory, 81*, 155.